Experimental investigation of interface states in photonic crystal heterostructures

Jiyong Guo, Yong Sun, Yewen Zhang, Hongqiang Li, Haitao Jiang, and Hong Chen*
Pohl Institute of Solid State Physics, Tongji University, Shanghai, 20092, People's Republic of China
(Received 27 March 2008; revised manuscript received 13 May 2008; published 18 August 2008)

Optical Tamm states, a kind of interface modes, are also called Tamm plasmon-polaritons. They are experimentally observed in photonic heterostructures based on microstrip transmission lines. The position of optical Tamm states can be designed exactly under effective impedance match and effective phase shift match conditions. Our results show that the photonic band gaps can have the effect of negative-permittivity or negative-permeability media in constructing the interface modes. The simulations and experimental results agree with each other quite well.

DOI: 10.1103/PhysRevE.78.026607 PACS number(s): 41.20.Jb, 42.70.Qs, 78.20.Ci, 73.20.Mf

I. INTRODUCTION

Photonic crystals (PCs), which have very broad application prospects in optics, have become one of the most popular topics in recent decades [1–3]. PCs possess photonic band gaps (PBGs) within which the propagation of electromagnetic (EM) waves will be blocked and they become evanescent waves. Because of PBGs, surface waves appear in PCs. The surface waves in one-dimensional photonic crystals (1DPCs) have already been studied by many methods [4–8]. Recently, a special type of lossless interface modes, called optical Tamm states (OTSs) in analogy with the Tamm states in solid state physics for electrons at crystal boundaries [9], has attracted much attention for potential applications due to their special advantages in polariton laser fabrication [10,11]. Tamm states are localized electronic states formed at the edge of a truncated periodic atomic potential [9]. The terminated solid introduces additional perturbation to the periodic potential and causes an asymmetric potential at the surface. The perturbation to the potential of surface atoms causes a localized state in the solid surface that is called the Tamm state. In analogy to the atomic potentials in the solid, the periodic impedances in a PC could be considered as optical potentials. One case of Tamm surface states in a finite chain of defects in a PC has been studied in detail [12]. Moreover, a photonic heterostructure composed of two kinds of PCs (or a PC and a homogeneous material) can offer asymmetric optical potentials in the interfaces of two different PCs (or a PC and a homogeneous material), leading to localized states in the interfaces. The interface state in photonic heterostructures and the Tamm state in solids both are caused by the asymmetric potential of a terminated periodic structure. So physically the interface states studied are analogous to the Tamm states in solids and could be called optical Tamm states [10,11]. OTSs lie in the overlap of the original band gaps of the two parts of the heterostructure and remain localized for any value of the in-plane wave vector (including the zero wave vector) [10,11]. EM waves that are incident on the structure can directly excite OTSs, which would be very convenient in real applications. In addition to dielectric PCs, the same possible EM states at the interface of a metal and a dielectric Bragg mirror (i.e., a 1DPCs) have also been discussed and the authors call them Tamm plasmon-polaritons (TPPs) [13]. Generally, PCs have been suggested to obtain a new EM interface mode that could confine EM energy strongly at the boundary. However, the details of how to design real heterostructures have not been presented clearly so far. Here we present an accurate and convenient way of designing OTSs using finite PCs, and the physical mechanisms involved are also discussed.

Besides the OTSs realized in PCs, similar interface modes have been found to appear in a paired structure composed of an ε-negative (ENG) material ($\varepsilon<0$, $\mu>0$) and a μ-negative (MNG) material ($\varepsilon>0$, $\mu<0$) (two kinds of single-negative metamaterials) [14–16]. The EM waves in an ENG or MNG material are evanescent waves since their wave vectors are complex. However, when an ENG material is paired with a MNG material, an interface mode with unit transmittance will appear under impedance matching and phase shift matching conditions [14–16]:

$$\mathrm{Im}(z_{\mathrm{ENG}}) = -\mathrm{Im}(z_{\mathrm{MNG}}), \tag{1}$$

$$\mathrm{Im}(k_{\mathrm{ENG}})d_{\mathrm{ENG}} = \mathrm{Im}(k_{\mathrm{MNG}})d_{\mathrm{MNG}}. \tag{2}$$

In Eqs. (1) and (2), z_{ENG} and z_{MNG} are the characteristic impedances of the ENG and MNG material, respectively, and k_{ENG} and k_{MNG} are the corresponding wave vectors. Im means the imaginary part, d_{ENG} and d_{MNG} are the thicknesses of the ENG and MNG material, respectively. These matching conditions are also equivalent to $\bar{\varepsilon}=0$, $\bar{\mu}=0$, where $\bar{\varepsilon}$ and $\bar{\mu}$ represent the volume-averaged permittivity and permeability of the whole heterostructure, respectively [15,16].

Similar to the waves in an ENG or MNG material, the EM waves with frequencies inside PBGs of PCs are also evanescent waves because the Bloch wave vectors are complex. So, within PBGs, PCs may have the effect of an ENG or MNG material when they are used to realize OTSs. Based on this hypothesis, the properties of PCs are described by their effective parameters that are calculated from the reflection and transmission coefficients [17]. Here the calculation only considers the holistic EM response [18].

In this paper, an interface mode at the boundary between a 1DPC and an ENG or MNG material is observed at a certain frequency when the matching conditions are satisfied. The evanescent waves in the ENG or MNG material are

*Corresponding author. honchenk@online.sh.cn

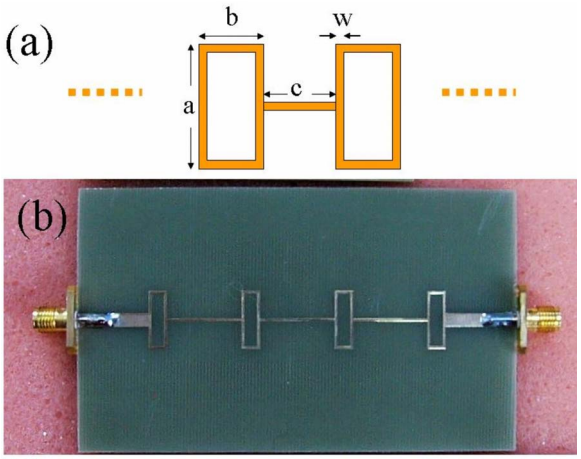

FIG. 1. (Color online) 1DPC fabricated by etching rectangular rings on microstrip. (a) Sketch of microstrip PC. $a=13.0$ mm, $b=4.0$ mm, $c=17.0$ mm, and $w=0.5$ mm. The substrate is FR-4 with a thickness of $h=1.6$ mm and the relative permittivity $\varepsilon=4.75$. (b) Photograph of the real structure.

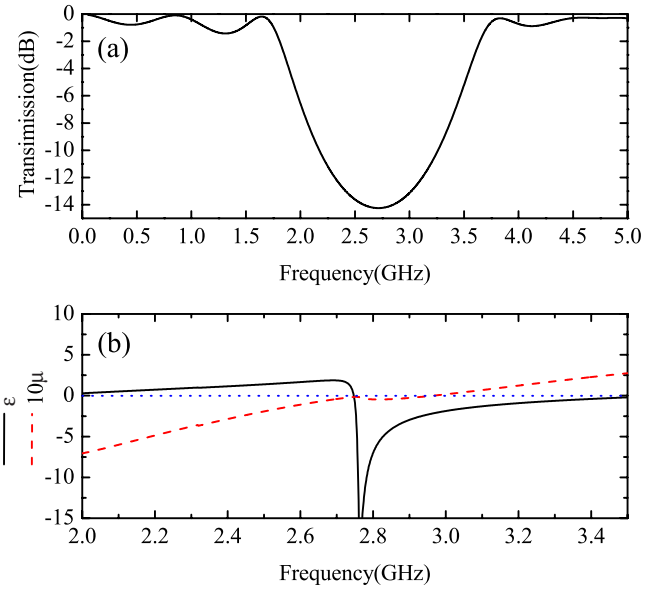

FIG. 2. (Color online) (a) Transmission of the PC with the parameters in Fig. 1. (b) Effective parameters within the band gap of the PC where the permittivity (permeability) is negative and permeability (permittivity) is positive. The permittivity (permeability) is shown by the solid black (red dashed) line. The value of the vertical axis of the horizontal blue dotted line is zero.

amplified in the 1DPC. The OTSs can also be designed simply at the boundary between two different 1DPCs (one has the effect of an ENG material while the other of a MNG material). Transmissions are enhanced at the predicted frequency in both simulation and measurement for all three kinds of heterostructures. Although the experiments were carried out in the microwave regime and only 1DPCs are considered, this approach may be extended to the infrared and visible wavelength regimes as well as to two- or three-dimensional cases. To the best of our knowledge, there are few works on the experimental realization of OTSs. In particular, we show that OTSs can be accurately and effectively designed by the matching conditions in finite PCs. The paper is organized as follows. In Sec. II, a real microstrip PC is described and the effective parameters of the band gap are retrieved by standard methods. In Sec. III, the OTSs are realized experimentally in three different types of heterostructures based on microstrip lines. Finally, a discussion and conclusion are given in Sec. IV.

II. THE BAND GAP PROPERTIES OF 1DPCS

A schematic of a microstrip PC is shown in Fig. 1(a). By constructing some periodic structures along a transmission line, one can obtain a quasi-1D PC in the microwave regime, i.e., a microstrip PC [19], which is widely used in the engineering field [20–24]. Microstrip lines provide us a good platform to study the properties of PCs in the microwave regime. In this paper heterostructures based on microstrip lines are used to form OTSs. Figure 1(b) shows a photograph of a real quasi-1D microstrip PC made on a flame retardant (FR)-4 substrate with a thickness of $h=1.6$ mm and a relative permittivity of $\varepsilon=4.75$. There is an earth plate on the bottom layer of printed circuit board (PCB). Rectangular rings and metallic lines are distributed alternately on the top layer. The structural parameters are follows: $a=13.0$ mm, $b=4.0$ mm, $c=17.0$ mm, w=0.5 mm, where a and b are the outside length and width of the rectangle, respectively, c is the length of the junction line, and w is the uniform width of the line. A section of 50 Ω microstrip line connecting the port is added to both ends for measurements.

Reflection and transmission coefficients needed for the retrieval of effective parameters are obtained through simulation by the advanced design system (ADS) of Agilent. Then, based on the reflection and transmission coefficients, the effective permittivity ε and permeability μ are determined [17], as well as the effective impedance z and effective phase shift kd of the 1DPC. Figure 2 shows that the 1DPC with the parameters in Fig. 1 has effective single-negative parameters in the band gap. The MNG parameter is located in the lower-frequency range while the ENG parameter is located in the higher-frequency region. In addition, we note there is one small region in the band gap where both the effective permittivity ε and permeability μ are negative. We think this is caused by the instability of the retrieval process in this region. The value of the effective permeability μ is very small and the effective permittivity ε is large. The impedance of this small region is near zero [as shown in Fig. 5(a), black solid line]. This will bring considerable instability and error in the effective parameter retrieval process.

Recently, an LC-loaded transmission line (TL) was introduced to construct metamaterials including double-negative materials ($\varepsilon<0$, $\mu<0$), ENG materials and MNG materials [25,26]. A six-unit effective ENG transmission line was manufactured to match the PC in Fig. 1, as shown in Fig. 3. The following parameters were chosen by careful adjustment: $L=2.2$ nH, $C=3.0$ pF, $d=5.4$ mm. This is because the values of lumped elements are discrete and optimization is needed based on the matching conditions. Similarly, an effective MNG transmission line matching the PC can also be

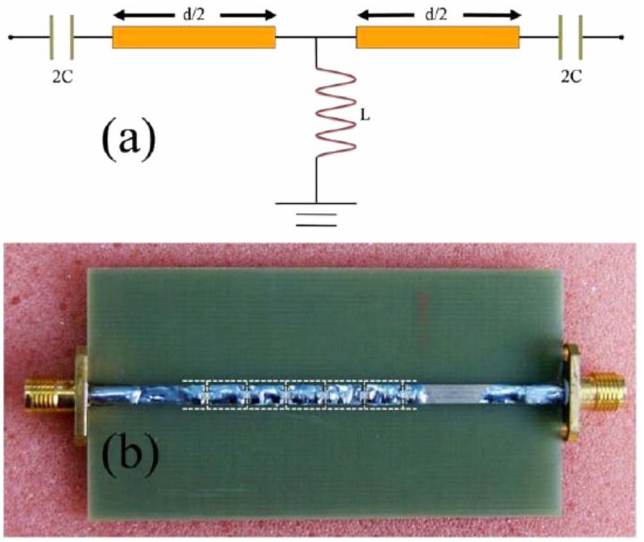

FIG. 3. (Color online) Effective ENG transmission line fabricated by loading lumped series capacitors and shunt inductors. (a) The circuit model of a unit cell with the loading lumped series capacitors $C=3.0$ pF, shunt inductor $L=2.2$ nH, and $d=5.4$ mm. (b) Photograph of a six-unit ENG transmission line. The white dashed line shows the position of every unit. Each end is a half unit and they constitute one unit. This structure is a little different from the sketch. However, they have similar transmission properties and the structure used here only needs one kind of capacitor.

designed by choosing the proper series capacitance C and shunt inductance L elements and the length of the unit cell d. The details will be discussed later.

Again, the effective permittivity ε and permeability μ of the effective ENG transmission line are determined from the reflection and transmission coefficients. Based on ε and μ, the effective impedance z and phase shift kd can be obtained. Figure 4 shows that there is an ENG region from 2.2 to 3.3 GHz for the structure in Fig. 3. These kinds of structures have been intensively studied in Ref. [26].

III. OTSS IN THREE TYPES OF HETEROSTRUCTURES

For the PC with parameters of Fig. 1 and the ENG transmission line with parameters in Fig. 3, we calculated the imaginary parts of the effective impedances and the effective phase shifts, respectively, as shown by the solid black lines and the red dashed lines in Fig. 5. At frequency 2.47 GHz where the PC shows the effect of a MNG medium, the matching conditions [Eqs. (1) and (2)] are satisfied, as indicated by the dotted lines in Fig. 5. So an OTS should occur at 2.47 GHZ for the paired structure composed of a PC and an ENG transmission line that is shown by Fig. 6(a). This prediction has been demonstrated in transmission spectra simulated by ADS and measured by an Agilent 8722ES. In Fig. 6(b), the transmission spectra of a PC, an ENG transmission line, and the paired structure are shown by the blue dotted lines, the red dashed lines, and the solid black lines, respectively. For the paired structure, a localized mode appearing in the frequency gap is at frequency 2.47 GHz for simulation and 2.57 GHz for experimental measurement, as

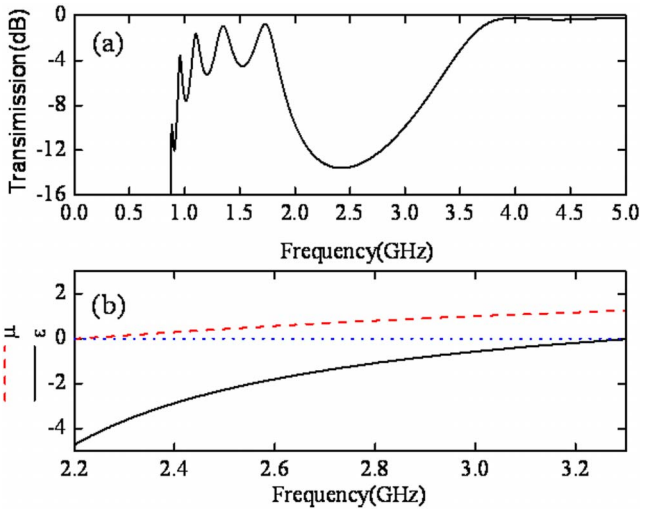

FIG. 4. (Color online) (a) Transmission of the effective ENG transmission line with the parameters in Fig. 3. (b) The corresponding effective parameters where the permittivity (the black solid line) is negative and the permeability (the red dashed line) is positive. The value of the vertical axis of the horizontal blue dotted line is zero.

indicated by the green dotted lines. The simulation and measurement agree quite well considering the fact that using the effective parameters for PC is an approximation. In addition the tolerance in fabrication and material absorption are other factors for discrimination. This localized mode is one kind of interface state since the EM fields exponentially decay from the interface of two media to both ends of the media (one example will be shown in detail later).

Based on the same method, a PC paired with an effective MNG transmission line is designed and manufactured with the following parameters: $a=16.0$ mm, $b=8.4$ mm, $c=12.6$ mm, $w=0.5$ mm, $L=8.2$ nH, and $C=1.5$ pF. The con-

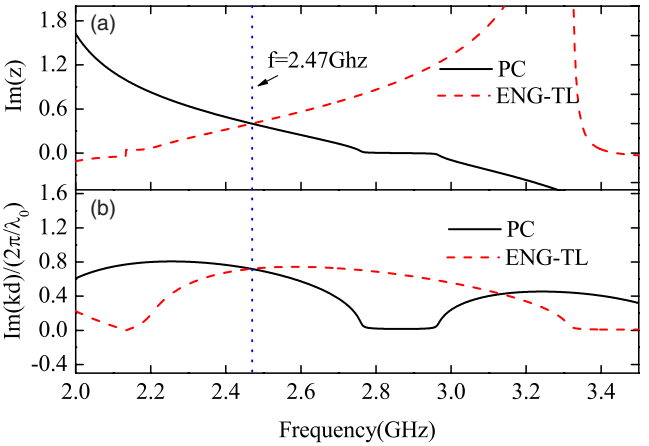

FIG. 5. (Color online) (a) Imaginary parts of the effective impedance of PC (the solid black line) and the ENG transmission line (the red dashed line). The sign of the imaginary parts of the ENG transmission line has been reversed. The matched point is at 2.47 GHz. (b) Imaginary parts of the effective phase shift of the PC (the solid black line) and the ENG transmission line (the red dashed line). λ_0 is the wavelength of the incident wave.

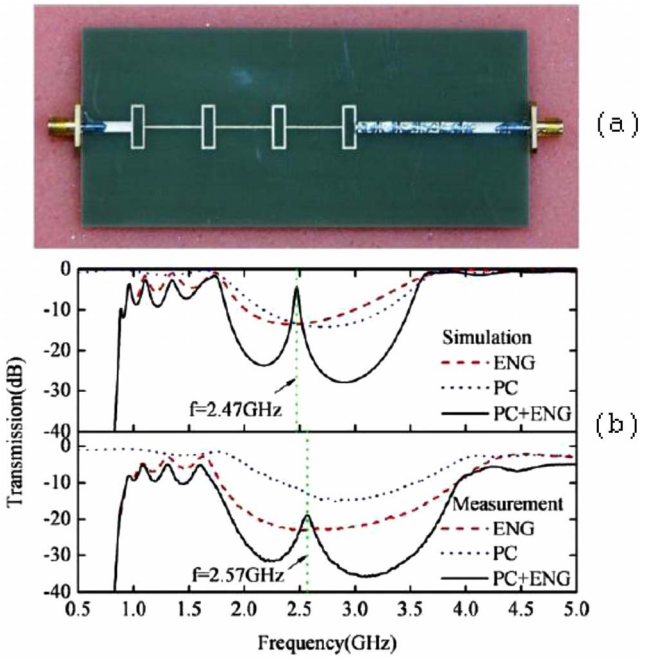

FIG. 6. (Color online) (a) Photograph of a paired structure composed of an ENG transmission line and a PC. (b) Simulated and measured results of transmissions of the ENG transmission line (the red dashed line), the PC (the blue dotted line), and the paired structure (the solid black line). The frequency of the localized mode is 2.47 GHz in simulation and 2.57 GHz in measurement.

figuration of an effective MNG transmission line is similar to that of an effective ENG transmission line, only the values of the lumped capacitor and the inductor being changed. The designed OTS is at 2.8 GHz under the matching conditions (the relevant matching parameter diagram is not shown because it is similar to Fig. 5). In Fig. 7, the transmission spectra of a PC, an MNG transmission line, and the paired structure are shown by the blue dotted lines, the red dashed lines, and the solid black lines, respectively. A localized mode with high transmission has also been observed at

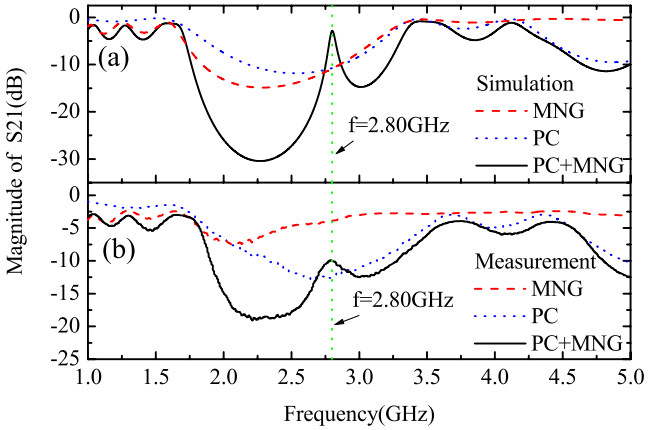

FIG. 7. (Color online) Simulated and measured results of transmissions of a MNG transmission line (the red dashed line), a PC (the blue dotted line), and their paired structure (the solid black line). The frequency of the localized mode is 2.8 GHz for both simulation and measurement.

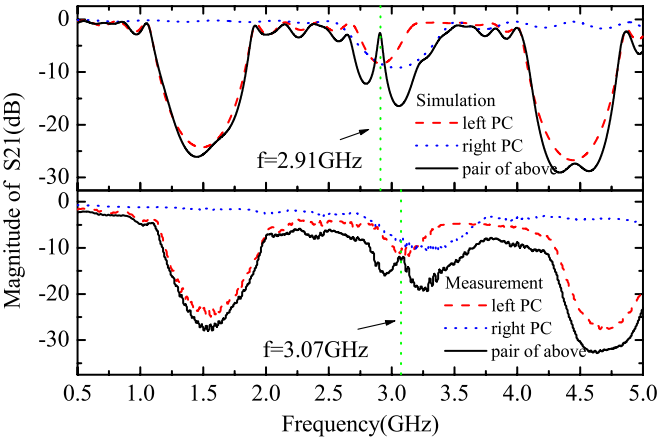

FIG. 8. (Color online) Simulated and measured results of transmissions of left PC (the red dashed line), right PC (the blue dotted line), and their paired structure (the black solid line). The frequency of the localized mode is 2.91 GHz in simulation and 3.07 GHz in measurement.

2.80 GHz in both simulation and measurement, as indicated by the green dotted lines. It should be pointed out that the previous PC in Fig. 1 can also have the effect of an ENG medium at frequency 2.8 GHz. But the effective MNG transmission line that matches the previous PC cannot be easily obtained because the values of the lumped components are

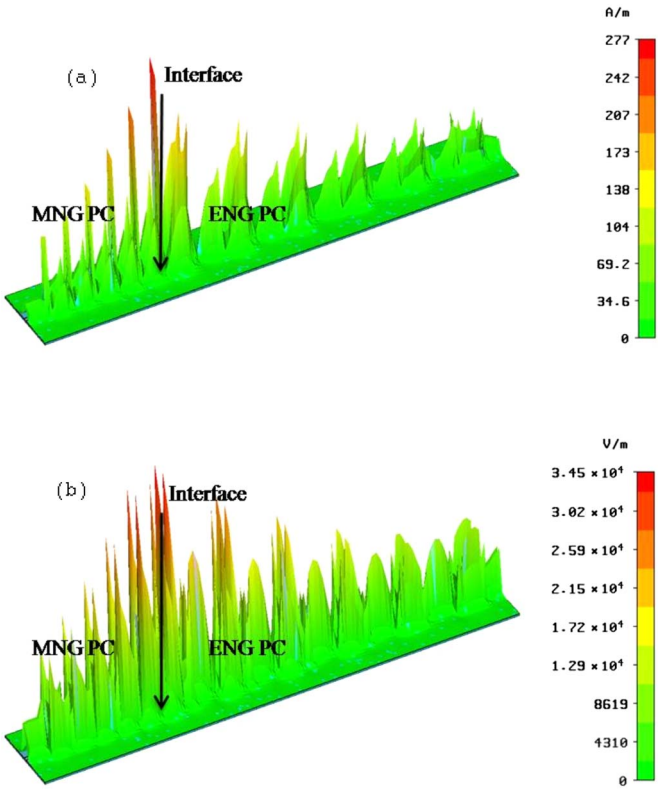

FIG. 9. (Color online) Field amplitude on the surface of PCB for a paired structure composed of two different PCs in Fig. 8 at matched frequency 2.91 GHz. The solid arrows indicate the interfaces and the right color bar denotes the strength scale. The (a) magnetic and (b) electric field distribution.

limited. So we designed a new PC that can easily match the effective MNG transmission line.

In addition to the heterostructures composed of a PC and an effective ENG or MNG transmission line, a heterostructure consisting of two different PCs can also have OTSs if one PC produces the effect of an ENG medium and the other that of a MNG medium. The parameters of the left PC equivalent to a MNG medium are as follows: $a_1=12.4$ mm, $b_1=14.2$ mm, $c_1=3.7$ mm, $w_1=0.3$ mm. Meanwhile, the parameters of the right PC equivalent to an ENG medium are as follows: $a_2=13.0$ mm, $b_2=21.0$ mm, $c_2=26.0$ mm, $w_2=0.5$ mm. These two different PCs satisfy the matching condition at 2.91 GHz. In Fig. 8, the transmission spectra of the right PC, the left PC, and the paired structure are shown by the blue dotted lines, the red dashed lines, and the solid black lines, respectively. For the paired structure, a localized mode is at 2.91 GHz in simulation and 3.07 GHz in the experimental measurement, as indicated by the green dotted lines. Besides the transmission spectra, the field maps simulated by computer simulation technology (CST) microwave studio show that this localized mode is indeed an interface mode that decays exponentially from the interface to the surrounding media. Figures 9(a) and 9(b) show the profile of the magnetic field and electric field of the OTS, respectively. It is seen that the EM energy is localized around the interface of the two different PCs. In fact, a strongly localized field is highly desirable in applications. The strength of the interface field could be enhanced by increasing the interface perturbation, as described in Ref. [12]. The deeper the position of the interface state in the gap, the higher is the strength of the interface field. In our paper, it is possible to choose another set of parameters to move the position of the interface state into a deeper position in the gap to obtain a stronger interface field. Of course, the absorption might affect the strength of localization, and careful optimization is needed for a better result.

The experiments above have shown that PCs in band gaps can create the effect of a MNG medium in a certain frequency range and an ENG medium in another frequency region. Then, under the condition of effective impedance matching and phase matching, we obtained OTSs in three different kinds of heterostructures involving PC(s). The experimental results agree with simulations quite well. The Bloch decaying waves in the gaps of PCs play an important role in the formation of OTSs.

IV. CONCLUSION

In conclusion, three kinds of heterostructures involving PC(s) are constructed in order to observe special interface modes, so-called optical Tamm states or Tamm plasmon-polaritons. The effective impedance match and effective phase shift match conditions provide us an accurate way to design desired OTSs in applications. All the OTSs are illustrated by both simulations and experiments that agree with each other quite well. Although the experiments were carried out in the microwave regime and only 1DPCs were considered, this approach may be extended to the infrared and visible wavelength region, as well as to two- or three-dimensional cases. Related work is ongoing. We hope these results are helpful for research into surface modes in PCs and related applications.

ACKNOWLEDGMENTS

This research was supported by CNKBRSF (Grant No. 2006CB921701), by CNSF (Grants No. 10634050 and No. 10704055), by Shanghai Science and Technology Committee.

[1] E. Yablonovitch, Phys. Rev. Lett. **58**, 2059 (1987).
[2] S. John, Phys. Rev. Lett. **58**, 2486 (1987).
[3] K. Busch, S. Lölkes, R. B. Wehrspohn, and H. Föll, *Photonic Crystals—Advances in Design, Fabrication, and Characterization* (Wiley-VCH, Weinheim, 2004).
[4] P. Yeh, A. Yariv, and C.-S. Hong, J. Opt. Soc. Am. **67**, 423 (1977).
[5] P. Yeh, *Optical Waves in Layered Media* (Wiley, New York, 1988).
[6] F. Ramos-Mendieta and P. Halevi, J. Opt. Soc. Am. B **14**, 370 (1997).
[7] F. Villa, J. A. Gaspar-Armenta, and F. Ramos-Mendieta, Opt. Commun. **216**, 361 (2003).
[8] J. A. Gaspar-Armenta and F. Villa, J. Opt. Soc. Am. B **20**, 2349 (2003).
[9] I. Tamm, Phys. Z. Sowjetunion **1**, 733 (1932).
[10] A. V. Kavokin, I. A. Shelykh, and G. Malpuech, Phys. Rev. B **72**, 233102 (2005); A. P. Vinogradov, A. V. Dorofeenko, S. G. Erokhin, M. Inoue, A. A. Lisyansky, A. M. Merzlikin, and A. B. Granovsky, *ibid.* **74**, 045128 (2006).
[11] A. Kavokin, I. Shelykh, and G. Malpuech, Appl. Phys. Lett. **87**, 261105 (2005).
[12] N. Malkova and C. Z. Ning, J. Phys.: Condens. Matter **19**, 056004 (2007).
[13] M. Kaliteevski, I. Iorsh, S. Brand, R. A. Abram, J. M. Chamberlain, A. V. Kavokin, and I. A. Shelykh, Phys. Rev. B **76**, 165415 (2007).
[14] A. Alù and N. Engheta, IEEE Trans. Antennas Propag. **51**, 2558 (2003).
[15] H. Jiang, H. Chen, and S. Zhu, Phys. Rev. E **73**, 046601 (2006).
[16] G. Guan, H. Jiang, H. Li, Y. Zhang, H. Chen, and S. Zhu, Appl. Phys. Lett. **88**, 211112 (2006).
[17] D. R. Smith, S. Schultz, P. Markoš, and C. M. Soukoulis, Phys. Rev. B **65**, 195104 (2002).
[18] T. Decoopman, G. Tayeb, S. Enoch, D. Maystre, and B. Gralak, Phys. Rev. Lett. **97**, 073905 (2006).
[19] F. Falcone, T. Lopetegi, and M. Sorolla, Microwave Opt. Technol. Lett. **22**, 411 (1999).
[20] V. Radisic, Y. Qian, R. Coccioli, and T. Itoh, IEEE Microw. Guid. Wave Lett. **8**, 69 (1998).
[21] S. S. Oh, C. S. Kee, J. E. Kim, H. Y. Park, T. Kim, I. Park, and

H. Lim, Appl. Phys. Lett. **76**, 2301 (2000).
[22] N. C. Karmakar and M. N. Mollah, IEEE Trans. Microwave Theory Tech. **51**, 564 (2003).
[23] M. J. Freire, R. Marques, F. Medina, M. A. G. Laso, and F. Martin, Appl. Phys. Lett. **85**, 4439 (2004).
[24] Y. H. Li, H. T. Jiang, H. Li, H. Q. Li, Y. W. Zhang, and H. Chen, Appl. Phys. Lett. **88**, 081106 (2006).
[25] G. V. Eleftheriades, O. Siddiqui, and A. K. Iyer, IEEE Microw. Wirel. Compon. Lett. **13**, 51 (2003).
[26] Liwei Zhang, Yewen Zhang, Li He, Hongqing Li, and Hong Chen, Phys. Rev. E **74**, 056615 (2006).